Brain Tumour Image Segmentation Using Deep Networks

Submitted by:

Mahnoor Ali

(NUST-00000206273)

Supervisor:

Dr. Syed Omer Gilani

School of Mechanical & Manufacturing Engineering (SMME)

National University of Sciences & Technology (NUST)

Islamabad, Pakistan

2020

Brain Tumour Image Segmentation Using Deep Networks

A Thesis submitted in partial fulfillment of requirement for the degree of

Master of Sciences

In

Biomedical Sciences

By

Mahnoor Ali

(NUST-00000206273)

Supervised by:

Dr. Syed Omer Gilani

Thesis Supervisor's Signature: _____

School of Mechanical & Manufacturing Engineering (SMME)

National University of Sciences & Technology (NUST)

Islamabad-Pakistan

2020

FORM TH-4

Master Thesis Work

We hereby recommend that the dissertation prepared under our supervision by **Mahnoor Ali (**Registration No. **00000206273)**, Titled: **Brain Tumour Image Segmentation Using Deep Networks** be accepted in partial fulfillment of the requirements for the award of MS degree. Grade **A**

Examination Committee Members

Name: Dr. Asim Waris Signature: _____

Name: Dr. Mohsin Jamil Signature: _____

Name: Dr. Amir Sohail Kashif Signature: _____

Supervisor's Name: Dr. Syed Omer Gilani Signature: _____

Date: **12-Sep-2020**

_____ _____

Head of Department Date

COUNTERSINGED

Date: _____ _____ Dean/Principal

Declaration

I certify that this research work titled "*Brain Tumour Image Segmentation Using Deep Networks"* is my own work. The work has not been presented elsewhere for assessment. The material that has been used from other sources has been properly acknowledged / referred.

Mahnoor Ali

MS BMS 00000206273

Plagiarism Certificate (Turnitin Report)

This thesis has been checked for Plagiarism. Turnitin report endorsed by supervisor is attached.

Mahnoor Ali

00000206273

Thesis Supervisor:

Dr. Syed Omer Gilani

Copyright Statement

- Copyright in text of this thesis rests with the student author. Copies (by any process) either in full, or of extracts, may be made only in accordance with instructions given by the author and lodged in the Library of NUST School of Mechanical & Manufacturing Engineering (SMME). Details may be obtained by the Librarian. This page must form part of any such copies made. Further copies (by any process) may not be made without the permission (in writing) of the author.
- The ownership of any intellectual property rights which may be described in this thesis is vested in NUST School of Mechanical & Manufacturing Engineering (SMME), subject to any prior agreement to the contrary, and may not be made available for use by third parties without the written permission of the SMME, which will prescribe the terms and conditions of any such agreement.
- Further information on the conditions under which disclosures and exploitation may take place is available from the Library of NUST School of Mechanical & Manufacturing Engineering, Islamabad.

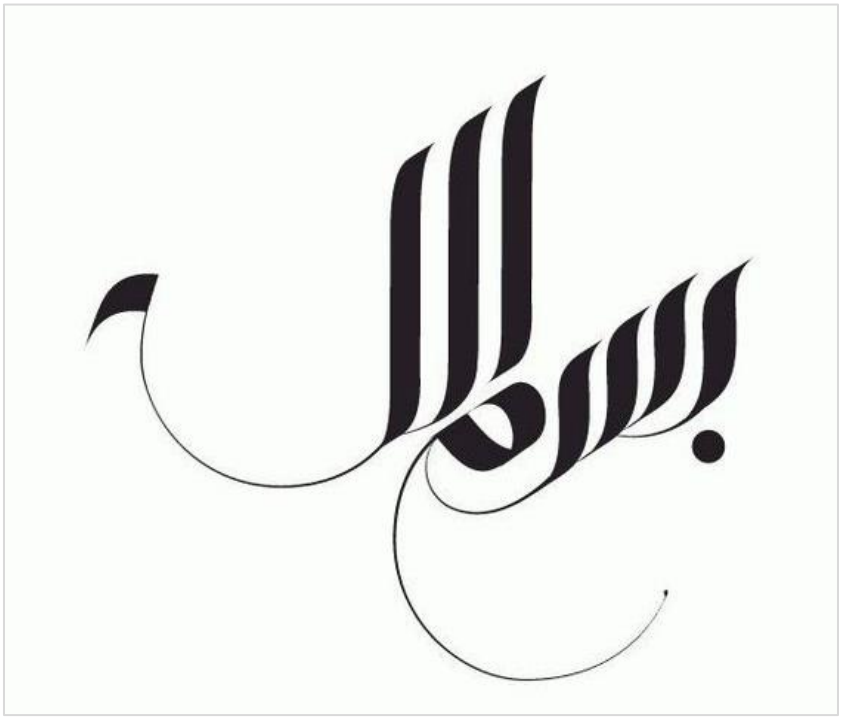

Dedicated to

mom & dad ♡

ACKNOWLEDGMENTS

"وَمَا تَوْفِيقِي إِلَّا بِاللهِ عَلَيْهِ تَوَكَّلْتُ وَإِلَيْهِ أُنِيبُ"

— "and my success can only come from Allah. In Him I trust, and unto Him I return."

Quran: Surah Hud [11:88]

I would like to thank my family, who stood by me and bore with me the many challenges that came with this work and offered their complete belief and support in every matter. My father, who believed in my success more than me, my mother, who prayed tirelessly and my brothers, who think me a genius when I am anything but. Thank you for being there.

I would also like to express my gratitude for my supervisor, Dr. Syed Omer Gilani, who made the impossible seem possible and offered his endless help. Special consideration to my GEC members Dr. Asim Waris, Dr. Mohsin Jamil and Dr. Amir Sohail Kashif for their presence and support.

I am highly grateful to my friend Rabbia Arshad for being with me in the long run, wherever life may take me. And my gratitude to Arsalan Asif, who inspired me with his faith to achieve more and be more.

Special thanks to friends such as Walifa Waqar, Mariam Fatima, Momina Hayat and Maria Ahmed, who checked on me without fail, needlessly asked after my wellbeing and kept me moving forward.

And my utmost thanks to my friends of late, Anum Hamid, Kashan Zafar, Naveed Malik and Zunaira Qureshi, for the many laughs and adventures. Thank you for everything.

- Mahnoor Ali.

CONTENTS

LIST OF ACRONYMS

BraTS	Brain Tumour Segmentation Challenge
CE	Cross Entropy
CNNs	Convolutional Neural Networks
DCAN	Deep Cascaded Attention Network
DL	Dice Loss
DMF	Dilated Multi-Fiber
DRLS	Deep Recurrent Level Set
DSC	Dice score coefficient
D-SEG	Diffusion Segmentation
DTI	Diffusion Tensor Imaging
ERTs	Extremely Randomised Trees
ET	Enhancing Tumour
FCN	Fully Convolutional Network
FL	Focal Loss
FLAIR	Fluid-Attenuated Inversion Recovery
GDL	Generalized Dice Loss
HGG	High-Grade Gliomas
LGG	Low-Grade Gliomas
MF	Multi-Fiber
ML	Machine Learning
MRI	Magnetic Resonance Imaging
nnU-Net	No-New-Net

RF	Random Forests
ROI	Region of Interest
SVM	Support Vector Machines
T1ce	T1 Contrast-Enhanced
T2	T2-Weighted
TC	Tumour Core
VAE	Variational Autoencoder
VLS	Variational Level Set
VOIs	Volume of Interests
WT	Whole Tumour

LIST OF FIGURES

LIST OF TABLES

LIST OF EQUATIONS

ABSTRACT

Automated segmentation of brain tumour from multimodal MR images is pivotal for the analysis and monitoring of disease progression. As gliomas are malignant and heterogeneous, efficient and accurate segmentation techniques are used for the successful delineation of tumours into intra-tumoural classes. Deep learning algorithms outperform on tasks of semantic segmentation as opposed to the more conventional, context-based computer vision approaches. Extensively used for biomedical image segmentation, Convolutional Neural Networks have significantly improved the state-of-the-art accuracy on the task of brain tumour segmentation. In this paper, we propose an ensemble of two segmentation networks: a 3D CNN and a U-Net, in a significant yet straightforward combinative technique that results in better and accurate predictions. Both models were trained separately on the BraTS-19 challenge dataset and evaluated to yield segmentation maps which considerably differed from each other in terms of segmented tumour sub-regions and were ensembled variably to achieve the final prediction. The suggested ensemble achieved dice scores of 0.750, 0.906 and 0.846 for enhancing tumour, whole tumour, and tumour core, respectively, on the validation set, performing favourably in comparison to the state-of-the-art architectures currently available.

CHAPTER 1

INTRODUCTION

INTRODUCTION

GLIOMAS

Accurate segmentation of tumours through medical images is of particular importance as it provides information essential for analysis and diagnosis of cancer as well as for mapping out treatment options and monitoring the progression of the disease. Brain tumours are one of the most fatal cancers worldwide and are categorized, depending upon their origin, into primary and secondary tumour types [1]. The most common histological form of primary brain cancer is the glioma, which originates from the brain glial cells [2] and attributes towards 80% of all malignant brain tumours [3]. Gliomas can be of the slow-progressing low-grade (LGG) subtype with a better patient prognosis or are the more aggressive and infiltrative high-grade glioma (HGG) or glioblastoma, which require immediate treatment [4]. These tumours are associated with substantial morbidity, where the median survival for a patient with glioblastoma is only about 14 months with a 5-year survival rate near zero despite maximal surgical and medical therapy [5]. A timely diagnosis therefore becomes imperative for effective treatment of the patients.

DIAGNOSTIC TOOLS

Magnetic Resonance Imaging (MRI) is a preferred technique widely employed by radiologists for the evaluation and assessment of brain tumours [1]. It provides several complimentary 3D MRI modalities acquired based on the degree of excitation and repetition times i.e. T1-weighted, post-contrast T1-weighted (T1ce), T2-weighted and Fluid-Attenuated Inversion Recovery (FLAIR). The highlighted subregions of the tumour across different intensities of these sequences [6], such as the whole tumour

(the entire tumour inclusive of infiltrative oedema), is more prominent in FLAIR and T2 modalities. In contrast, T1 and T1ce images show the tumour core exclusive of peritumoural oedema [7]. It allows for the combinative use of these scans and the complementary information they deliver towards the detection of different tumour subregions.

DEEP LEARNING

The Multimodal Brain Tumour Segmentation Challenge (BraTS) is a platform to evaluate the development of machine learning models for the task of tumour segmentation, by facilitating the participants with an extensive dataset of 3D MRI images of the gliomas (both LGG and HGG) and associated ground truths annotated by expert physicians. The provided multimodal scans are used for both training and validating the neural networks designed for the particular segmentation task [6], [8]–[11].

Manually delineating brain tumour subregions from MRI scans is a subjective task, and therefore it is time-consuming and prone to variability [12]. Automated segmentation of gliomas from multimodal MRI images can consequently assist the physicians to speed-up diagnosis and surgical planning as well as provide an accurate, reproducible solution for further tumour analysis and monitoring [13], [14]. The classical methods of automated brain tumour segmentation rely on feature engineering, which involves the extraction of handcrafted features from input images with follow up training of classifier [11], [15]. Unsupervised learning algorithms bypass the complexity in designing and selecting features by automatically learning a hierarchy of feature representations [16]–[19], with deep learning models excelling at the task [11]. Convolutional Neural Networks (CNNs) is regarded as the state of the

art methods for brain tumour image segmentation as they learn the most useful and relevant features automatically [6].

However, accurate segmentation of tumour remains a challenge; due to heterogeneity in terms of shape, size, and appearance of the gliomas as well as ambiguous and fuzzy boundary existing between cancer and brain tissue [20]. The intensity variability of the MRI data further adds to this difficulty [13]. Therefore, it is still open to improvement, allowing further exploration for better segmentation techniques and accuracy.

In this work, we utilise multiple 3D CNN models for brain tumour segmentation from multimodal MRI scans and ensemble their probability maps for more stable predictions. The networks are trained separately, with hyperparameters optimised for each model, on the training dataset acquired from the 2019 Brain Tumour Segmentation (BraTS) challenge. A rigorous evaluation on the BraTS validation set resulted with the proposed ensemble achieving dice scores of 0.750, 0.906 and 0.846 for enhancing tumour, whole tumour, and tumour core, respectively.

AIMS AND OBJECTIVES

The aim of the study is the proposition of an automated brain tumour segmentation method, for successful delineation of tumour into intra-tumoural classes with greater efficiency and accuracy.

The objectives include to:

- Develop an automated deep neural network that segments brain tumours from MRI scans with great accuracy.
- Train and test the proposed network on online available brain tumour dataset (BraTS-19 Dataset).
- Determine its efficiency in comparison to methods already implemented and available.

CHAPTER 2

LITERATURE REVIEW

LITERATURE REVIEW

Numerous research studies highlight the importance of machine learning (ML) to facilitate and improve the efficiency of human practices. From combining ML with ubiquitous computing [21] to employing it for foreign object detection [22], many techniques have emerged to automate otherwise challenging tasks. Pervasive as gliomas have become, it is imperative that they are monitored carefully and operated on, depending on the prognosis. Many ML algorithms can accurately segment the cancer regions and assist the neuroradiologists in disease monitoring and planning.

The data used for these techniques must illuminate the variable characteristics of the gliomas, from the tumour infiltrative growth patterns to their heterogeneity [23], to attain considerable accuracy during segmentation. A study demonstrates the use of multimodal MRI data in a tissue type mapping protocol that serves to identify the grade as well as acquire spatial information of the tumour [24]. Multi-sequence MRI data is also provided by the BraTS challenge, containing both HGG and LGG scans of multi-institute patients, to facilitate users for devising successful glioma delineation techniques [9]–[11].

MACHINE LEARNING FOR GLIOMA SEGMENTATION

Supervised learning techniques with discriminative classifiers have been used for accurate delineation of gliomas, of which the most successful are random forests (RF) and support vector machines (SVM). Soltaninejad *et al.* [25] initially devised an approach to classify brain tumours grades using superpixels generated through bi-modal MRI data of patients, particularly by using FLAIR and T2-weighted MR data. The mean intensity of the superpixels was utilised to obtain the region of interest (ROI)

from which the 1st and 2nd order feature representations were extracted and passed onto the SVM classifier to delineate and differentiate between tumour grades. They continued down this avenue of research, and worked further with superpixels, acquired using mono-modal MRI data of patients [26]. After their segmentation from the FLAIR-MRI, statistical and textural features were extracted from these voxel-wise class labels, which were then fed into the extremely randomised trees (ERT) as well as the SVM classifier to ascertain whether the voxels represented healthy or tumoural brain regions. The method performed well on BraTS 2012 dataset, with the classification results compared to show that ERT works marginally better than SVM on detection and segmentation of the tumour grades.

Expounding on their earlier work, Soltaninejad *et al.* [27] employed multi-sequence MRI images, along with diffusion tensor imaging (DTI) data, to obtain 3D superxovels which provide clear tumour boundaries across the image modalities. The extracted texton and intensity-based statistical features were given to the RF classifier to classify the voxels. Inclusion of DTI components (isotropic (p) and anisotropic (q)) with the conventional MRI data resulted in considerable improvement of classification results. The method performed well and provided expert segmentations of the tumours when tested on the BraTS 2013 dataset. However, they are not the first to have utilised DTI for refined tumour segmentation. Jones *et al.* [28] suggested the use of diffusion characteristics to semi-automatically segment lesions from volumetric MRI data in a method termed as diffusion segmentation (D-SEG). After appropriating the voxels in the (p, q) space into clusters through k-means clustering, the boundaries segregating the healthy brain tissue and tumour regions are made apparent and clear in the resulting tissue segments. This information is utilised to extract the volume of interests (VOIs)

from which the D-SEG spectrum is calculated, representing the variable proportion of diffusion within the VOIs. The spectra are then classified through SVM to achieve considerable classification accuracy.

DEEP LEARNING ARCHITECTURES FOR TUMOUR SEGMENTATION

Deep learning algorithms outperform on tasks of semantic segmentation as opposed to the more conventional, context-based computer vision approaches [29]. Extensively used for biomedical image segmentation, the Deep Convolutional Neural Networks have carved out a niche for achieving the state of the art accuracy on the task of brain tumour segmentation [30]–[35].

A 2D U-Net architecture was put forth for the automated segmentation of brain tumour [36]. For increased network efficiency, various data augmentation techniques were applied along with the soft dice loss function to mitigate the class imbalance issue in the data. Fidon *et al.* [37] refined a neural network previously used for the task of brain parcellation and adapted it for multimodal MRI data input. ScaleNet made use of a merging operation in place of concatenation to connect the frontend and backend of the network, thereby allowing it to be scalable and generalised. Le *et al.* [38] designed an architecture which combined the standard variational level set (VLS) with a fully convolutional network (FCN). The new model referred to as the deep recurrent level set (DRLS), performed well in segmenting the tumour in comparison to the other models of the time, improving the otherwise rudimentary VLS into a deep learnable framework. Y. Qin *et al.* [39] introduced the autofocus layer, which enhanced the multi-scale processing of network and learned through an attention mechanism to select the optimal scale for object identification in medical images. The dilated

convolution layer improved the interpretability and representation capacity of the network leading to improved tumour segmentation.

A fully convolutional network (FCN) was suggested by Shen *et al.* [40], trained to learn boundary and region tasks, and successfully extracted contextual information from MRI scans with considerably low computation cost. Working with a similar architecture, Pereira *et al.* [41] set forth an FCN which captured more sophisticated features through feature recombination and also introduced a recalibration block in the structure. Zhou *et al.* [42] proposed a multi-task CNN, which integrated and trained on the different tasks of brain tumour segmentation in terms of their correlation and simplified the inference process through a one-pass computational scheme. Ji *et al.* [43] proposed a weakly-supervised U-Net that employed a scribble-based approach. They initially trained the network on whole tumour scribbles before exposing it to global labels for accurate substructure segmentation. Another network is trained on the results of the previously trained U-Net to segment the enhancing tumour and tumour core. Xu *et al.* [44] introduced this 3D deep cascaded attention network (DCAN), which is more straightforward in complexity compared to other cascaded models. It dealt with the multi-class segmentation task through separate branches and a shared feature extractor between them. It extracted the correlational information between the sub-regions through a cascaded attention method for guidance.

Brain Tumour Image Segmentation (BraTS) Challenge 2018

Myronenko [45] ranked first among the top submissions of the BraTS 2018 challenge with their encoder-decoder based CNN architecture. It augmented a variational autoencoder (VAE) for regularisation, allowing the reconstruction of original input images. During training, they used a crop size of 160x192x128 and a batch size of 1,

with no additional training dataset employed. The method proposed by Isensee *et al.* [46] placed second in the same challenge with minor alterations made to the original U-Net architecture. The 3D U-Net, or the no-new-Net (nnU-Net) as named by the authors, replaced ReLU activation functions with leaky ReLU and instance normalisation with batch normalisation. The training performed with an image patch size of 128x128x128 and batch size of 2. The same architecture, trained from scratch with changed hyperparameters, is expanded and used as part of our ensemble as well. Working with a U-Net like structure, McKinley *et al.* [47] incorporated dilated convolutions into the DenseNet architecture and trained with a newly formulated label certainty loss function. The tensor fed into the network was of the dimensions $2 \times 4 \times 5 \times 192 \times 192$, with the batch size of 2. Another noteworthy model is ensemble proposed by Zhou *et al.* [48] which consisted of various improved CNN architectures (previously used by them as mentioned above) trained to learn contextual information that served to produce robust predictions.

In this study, we propose an ensemble of two networks; a 3D CNN and a U-Net, in a different yet straightforward combinative technique that results in better and accurate predictions in comparison to uniform weighting. The task is to develop an automated brain tumour segmentation method, for successful delineation of tumours into intra-tumoural classes with improved efficiency and accuracy in comparison to existing methods. Our proposed model shows comparable, and in some cases, improved results to the state-of-the-art models.

CHAPTER 3

MATERIALS & METHODS

MATERIALS & METHODS

DATASET

We use the 2019 Brain Tumour Segmentation Challenge (BraTS) dataset [6], with the training set employed to train the models and the validation set for the evaluation of the proposed ensemble. The training set consists of 259 high-grade glioma and 76 low-grade glioma patients with expertly annotated ground truths. In contrast, the validation set includes 125 cases of unknown grade (the labels are not made available to the public) [8]–[11]. The data varies from that utilized in the prior years, more specifically data from 2016 and before as the labels of the corresponding images had not be manually annotated by experts. Rather, the labels were acquired through the coalescence of segmentations from the most successful of architectures of previous challenges.

The multi-institutional dataset, acquired from 19 different contributors, contains multimodal MRI scans of each patient, namely T1, T1 contrast-enhanced (T1ce), T2-weighted (T2), and Fluid Attenuated Inversion Recovery (FLAIR), from which the tumoural subregions are segmented. The data is processed to overcome discrepancies such that they are skull-stripped, aligned to match an anatomical template, and resampled at a resolution of $1mm^3$. Each sequence has a volume (dimension) of 240 × 240 × 155. Example images from the training set, as well as the corresponding ground truth, are shown in Figure 1. The manual ground truths (inclusive in the training set) highlight the three tumour regions: the peritumoural oedema, the enhancing tumour, and the necrotic and non-enhancing core

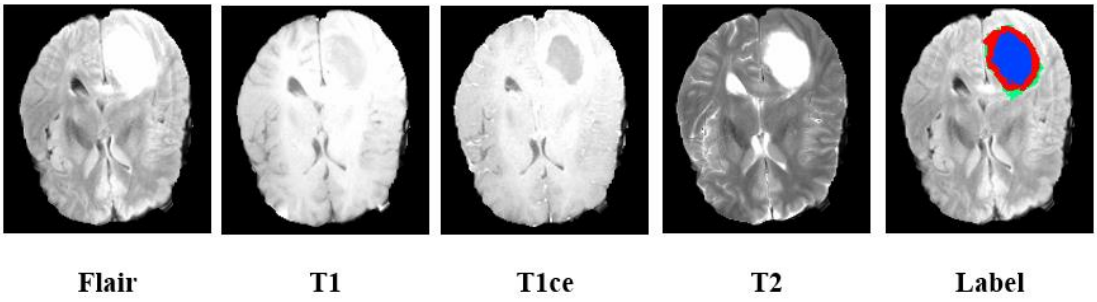

Figure 1. Image modalities of a single patient (HGG) in the BraTS-19 Training Set, along with the manual annotation overlaid on the Flair image.

As visualized in Figure 2, the manual annotations of the tumour include the background (label 0), necrotic and non-enhancing tumour (label 1), peritumoural edema (label 2) and GD-enhancing tumour (label 4). These labels are merged into three sub-regions: the whole tumour (label 1, 2 and 4), the tumour core (label 1 and 4) and the enhancing tumour (label 4). The segmentation accuracy (dice score metric) is measured for these regions [11].

Figure 2. Manually annotated ground truth with each of the individual tumour regions represented as separate labels.

No external dataset is used in the experiments. Additionally, access to the BraTS-19 test set is limited to the challenge participants only. Therefore, we report test results on the BraTS-19 validation set. We first report the segmentation results of the

proposed network on the validation set and later compare it to the existing state of the art architectures.

METHODOLOGY

Ensembling is often adapted for the task of brain tumour segmentation and has the advantage of improving both results and performance [47]–[49]. We propose a lightweight ensemble ((as generalized in Figure 3) consisting of as few as two networks, each selectively trained on the training set.

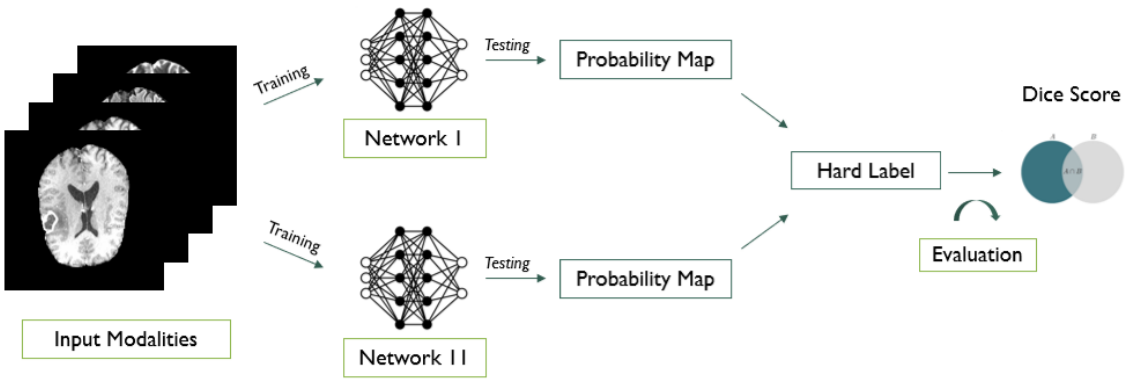

Figure 3. General Scheme of the work. Selected models are separately trained on the input MRI modalities and then tested to produce probability maps. These soft labels are selectively combined to generate the final hard prediction which is submitted online for further evaluation.

The outputs of these networks are segmentation map that differs in terms of segmented tumour sub-regions. The segmentation maps are then combined to get the final prediction. In the following sections, we provide further details on these two networks.

Network 1 (3D CNN)

The first model used in the ensemble is a 3D CNN, initially developed by Chen *et al.* [50]. It uses a multifiber unit (an array of 3D CNN, Figure 4) with weighted dilated convolutions to glean feature representation at multi-scale for volumetric

segmentation. The network showed good results on the BraTS 2018 Challenge. Extending on their work, we fine-tune the model for improved segmentation.

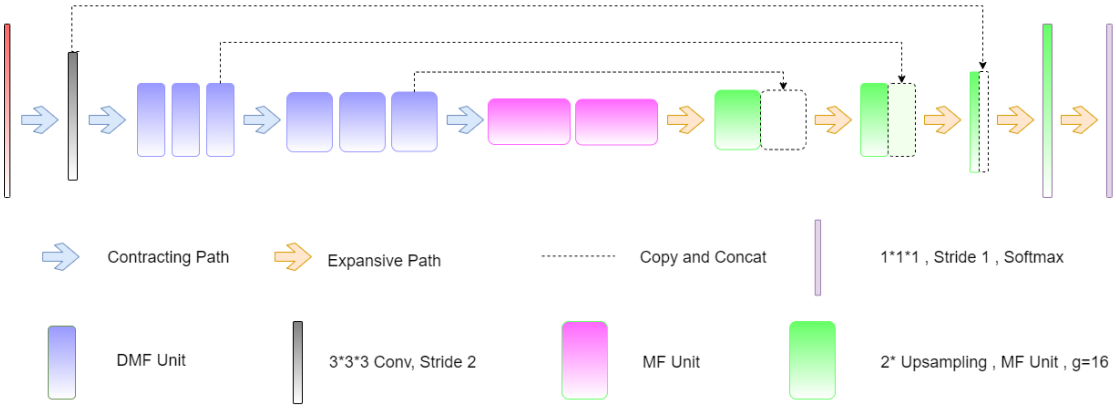

Figure 4. A schematic visualization of the 3D CNN architecture, where g represents the convolutional channels that are split into groups to reduce feature map connectivity. The multi-fiber (MF) blocks make use of a multiplexer allowing for the flow of information between groups. Each dilated multi-fiber (DMF) block is a dilated convolutional unit, with adaptive weighting, which serves to capture spatial information of the tumour.

Preprocessing: The data is augmented using a multitude of techniques (cropping, rotation, mirroring) before feeding it into the network for training.

Training: We trained the model for 150 epochs with a patch size of 128x128 and modified loss function, combining the generalised dice loss and the focal loss.

$$Loss = L_{GDL} + L_{FL} \quad (1)$$

Focal loss (FL) is employed in object detection and has shown to enhance accuracy while dealing with the issue of foreground imbalance [51], [52].

$$L_{FL} = -((1 - pt)^{\gamma}) \log pt \quad (2)$$

where, pt is the posterior probability and γ is the modulating hyperparameter set to 2.0.

Developed for the imbalance as occurs in certain rare tasks, the generalized dice loss (GDL) has been used to tackle the class imbalance problem that exists in the dataset [53].

$$L_{GDL} = 1 - 2\,\frac{\sum_{n=1}^{N} w_n \sum_i g_n^i\, p_n^i}{\sum_{n=1}^{N} w_n \sum_i (g_n^i + p_n^i)} \tag{3}$$

where, N represents the number of classes and w_n denotes the weight assigned. g_n and p_n are the voxel values for the ground truth and the predicted image, respectively, for class n.

The fine-tuned hyperparameters are shown in Table 1.

Table 1. Hyperparameters Used for CNN Training

Name	VALUE
Input Size	128 × 128 × 128
Batch Size	5
Learning Rate	1×10^{-3}
Optimizer	Adam
Epoch	150
Loss Function	L_{GDL} [a] + L_{FL} [b]

[a] L_{GDL} is the generalized dice loss.
[b] L_{FL} is the focal loss

Inference: We applied zero-padding to the MRI data so that the original 240 × 240 × 155 voxels are converted to 240 × 240 × 160, a depth which is divisible by the network. Once the data is ready for the inference, we pass it through the trained network to generate probability maps. The ensemble subsequently uses these maps for final prediction.

Network 2 (3D U-Net)

The second model of our ensemble is a 3D U-Net variant which is different from the classical U-Net architecture; ReLU activation function is replaced by leaky ReLUs and the use of instance normalisation in place of batch normalisation [46]. The network has shown comparable results on the medical segmentation benchmark, Medical Segmentation Decathlon, and BraTS 2018 Challenge. The model is trained from scratch on our dataset while having the same architecture (Figure 5) as reported in [46].

Preprocessing: We crop the data to reduce the size of the MRI slice. Afterwards, we resample the images along with median voxel spaces of the otherwise heterogeneous data followed by a z-score normalisation.

Training: For training the network, we use the input patch size of 128 × 128 × 128 voxels and batch size of 2. Different data augmentation techniques (rotation, mirroring and gamma correction) are applied on the data during runtime to circumvent overfitting and to enhance the segmentation accuracy of the model. The loss function combines the binary cross-entropy and the dice loss.

$$Loss = L_{dice} + L_{CE} \quad (4)$$

Dice loss (DL) is a derivative of the Dice score coefficient (DSC), employed to determine the measure of overlap between regions [54], which is particularly useful for segmentation problems where the labels are available.

$$L_{dice} = \frac{1}{|N|} \sum_{n \in N} \frac{2 \sum_i g_n^i p_n^i}{\sum_i (g_n^i + p_n^i)} \tag{5}$$

While the Cross Entropy (CE) loss maps out the probability distributions [55].

$$L_{CE} = -\sum_{n=1}^{N} g_n \log p_n \tag{6}$$

where, N is the number of classes and g_n and p_n are the voxel values for the ground truth and the predicted image, respectively.

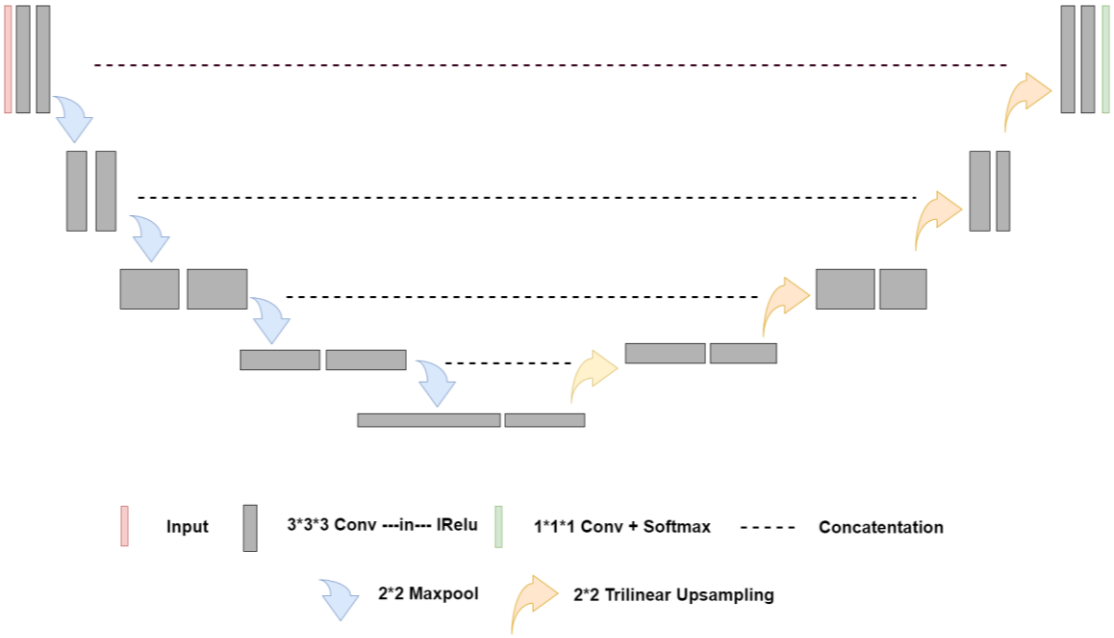

Figure 5. A schematic representation of the U-Net architecture. Inputs of patch size 128 × 128 × 128 are fed into the model. 3D convolutional blocks (as represented by grey boxes) are used with leaky ReLU function activations and instance normalization. Trilenaer upsampling is employed to achieve the output of the same spatial dimensions as that of the input.

Table 2 details the hyperparameters during training.

Table 2. Hyperparameters Used for CNN Training

Name	VALUE
Input Size	128 × 128 × 128
Batch Size	2
Learning Rate	3×10^{-4}
Optimizer	Adam
Epoch	150
Loss Function	$L_{dice} + L_{CE}$ [c]

[c] L_{CE} is the cross-entropy loss

Inference: Inference is a patch-based where all the patches overlap by half their size and the voxels near the centre have a higher weight attributed to them. Mirroring along the patch axes serves as additional data augmentation during the test time. The outputs are probability maps for the ensemble.

Ensembling

The ensemble is not built by simple averaging of the predictions (probability maps) generated by the two models. We merge the outputs of the two models after rigorously testing a strategy termed as *variable ensembling* (illustrated in Figure 6).

We separately test these trained networks on the validation set to obtain corresponding segmentation images. These predictions from the individual models are evaluated on the online BraTS server[1] independently to determine their efficiency in segmenting

[1] https://ipp.cbica.upenn.edu

the tumour regions successfully. We then compare the dice scores of the two models to identify which network is more accurate, and outperforms the other, for any specific tumour region.

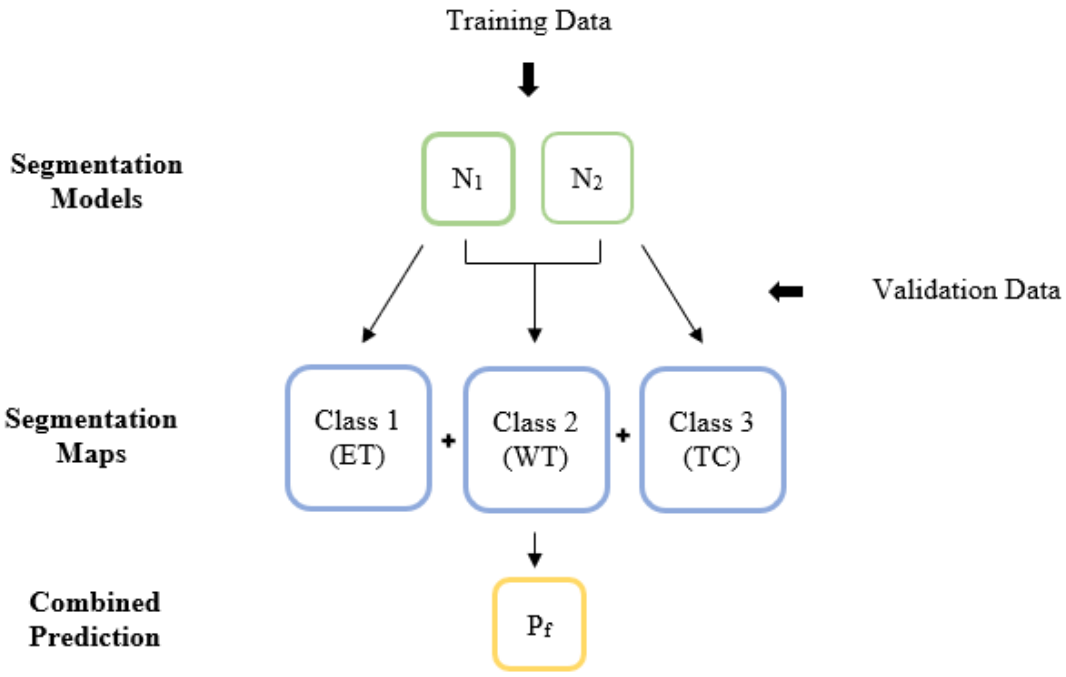

Figure 6. A general representation of the ensembling technique used to generate the final output. The 3D CNN (mentioned as N_1) more accurately segments the enhancing tumour (ET), while the 3D U-Net (mentioned as N_2) performs better for the tumour core (TC), therefore, the respective models' segmentation for that particular subregion are used in the final prediction (P_f). For the whole tumour (WT), both models contribute equally towards to the output.

Qualitative and quantitative (dice scores) results demonstrate that CNN performs better for segmenting the enhancing tumour. At the same time, the U-Net is more accurate for segmenting tumour core. However, in case of the whole tumour, combining the predictions from both networks (equally) outperforms the segmentation results independently. Therefore, to generate the final ensemble predictions for three regions; (1) tumour core, we used only U-Net's output (2) enhancing tumour, we used only CNN's output (3) the whole tumour, we equally weighed the output of both

networks. The predictions were evaluated on the online server to obtain the dice scores for the ensemble. We discuss these results in more detail in the next section.

.

CHAPTER 4

RESULTS

RESULTS

Here we present results from an ensemble of 2 networks, variants of a U-Net and a CNN, both selectively trained on the BraTS 2019 training set (n = 335) and tested on the provided BraTS 2019 validation set (n = 125). We then intelligently combine the segmentation maps from these models to give a final prediction for tumour tissue type as shown in Figure 7. The dice scores achieved by the ensemble (proposed) are 0.750 for enhancing tumour, 0.906 for the whole tumour, and 0.846 for tumour core**.**

Figure 7. Predictions of a single patient obtained separately through the models, as well as the final combinative prediction.

In Figure 8, we show the segmentation results of a single patient overlaid on the MRI Flair. The segmentation maps are generated from both models separately, and then the final merged output is shown. The dice score for the patient was 0.930, 0.949 and 0.927 for enhancing tumour, whole tumour, and tumour core, respectively.

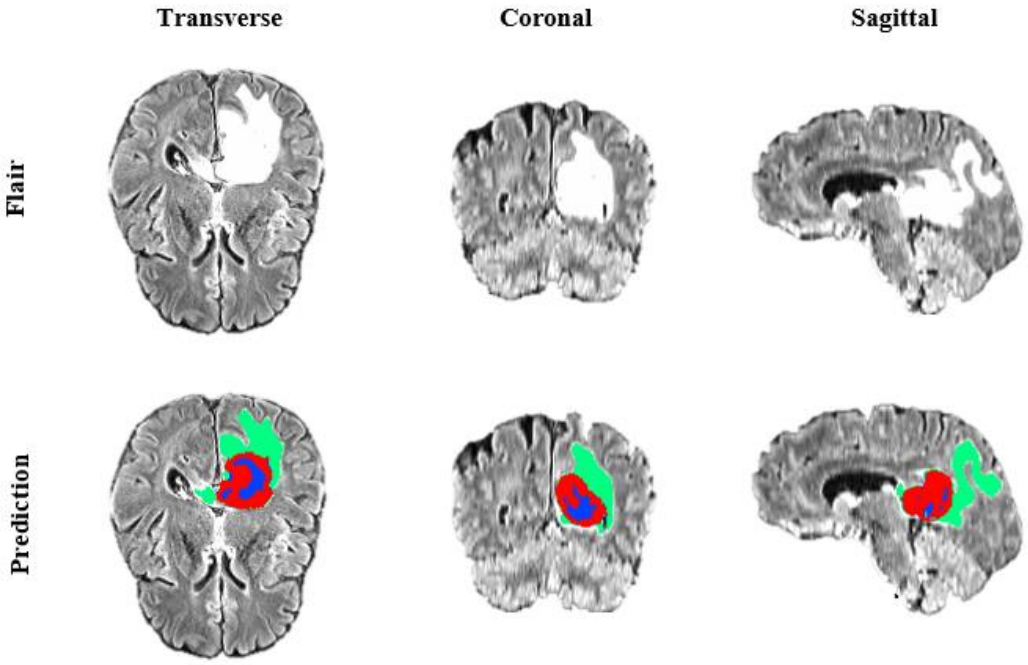

Figure 8. Example MRI Flair scan of a single patient exhibited from transverse, coronal and sagittal slices, overlaid with the segmentation prediction from the proposed model. The tumour regions are color coded, with the whole tumour representing all the segmentation classes in green, the tumour core including both the blue and red region, while the enhancing tumour is shown as the red region.

VARIABLE ENSEMBLING

We further analysed different ensemble techniques (as shown in Table 3) to determine if there is any difference between the methods and which of the two results in the most accurate of segmentations. As depicted in Table 3, the proposed ensembling scheme gives better accuracy in comparison to simple averaging.

Table 3. Performance (Dice Scores) Through Different Ensembling Efforts on BraTS-19 Validation Set

Strategy	ET	WT	TC
Simple Averaging	0.740	0.903	0.805
Variable Ensembling	0.750	0.906	0.846

COMPARISON WITH CHALLENGE PARTICIPANTS

We evaluated the proposed ensemble on the BraTS 2019 validation set and later compared it to top ranking architectures on the challenge website. Table 4 shows comparative dice scores obtained through the online BraTS server. The ensemble (proposed) achieved dice scores of 0.750, 0.906 and 0.846 for enhancing tumour, whole tumour, and tumour core, respectively.

Table 4. Performance (Dice Scores) in Comparison with Challenge Participants on BraTS-19 Validation Set

Authors	ET	WT	TC
Jiang *et al.* [56]	**0.802**	0.909	**0.864**
Zhao *et al.* [57]	0.754	**0.910**	0.835
McKinley *et al.* [58]	0.770	0.909	0.830
Proposed Method	0.750	0.906	0.846

The cascaded U-Net employed by Jiang *et al.* [56] achieved the best scores of the challenge, to which our results compare favourably, with significant performance gap occurring in terms of the enhancing tumour. Our ensemble gives improved results for the tumour core than the DCNN used by Zhao *et al.* [57] and just falls short for the

enhancing tumour with a minor performance gap. Similarly, it segments the tumour core with more accuracy as compared to CNN developed by McKinley *et al.* [58].

RESULT COMPARISON WITH DIFFERENT FRAMEWORKS

Table 5 shows the comparison with various state of the art methods (also validated on the BraTS 2019 dataset). Any of the other frameworks did not use additional data during training. Except for the enhancing tumour, the proposed ensemble results in better segmentations than the other available networks for both the whole tumour and tumour core, as evidenced by the dice scores.

Table 5. Performance (Dice Scores) in Comparison with Other Architectures on BraTS-19 Validation Set

Authors	ET	WT	TC
FCN [59]	0.766	0.896	0.790
Residual Inception Dense Networks [49]	0.779	0.897	0.784
U-Net [60]	0.787	0.896	0.800
3D Multi-Encoder/Decoder Network [61]	0.75	0.90	0.83
CNN [62]	**0.800**	0.894	0.834
Proposed Method	0.750	**0.906**	**0.846**

The promising performance by our simple ensemble of a U-Net and CNN is indicative of its efficiency and potential usability to achieve comparable and often better segmentation accuracy than its contemporaries.

CHAPTER 5

DISCUSSION

DISCUSSION

We propose an ensemble of a 3D U-Net and CNN for the task of brain tumour segmentation on multimodal MRI data. We combine the outputs of the two networks through variable ensembling to attain competitive classification accuracy on the BraTS 2019 validation set. Our proposed method performs favourably to state of the art methods by achieving mean dice scores of 0.750, 0.906 and 0.846 on enhancing tumour, whole tumour, and tumour core, respectively.

We experimented with a multitude of networks and their different combinations before deciding on the 3D U-Net and CNN. We also worked on different variants of CNN by changing the layers employed in the original architecture, but it did not result in improving the performance.

While our method performs favourably on the whole tumour and tumour core classes, the segmentation accuracy of the enhancing tumour needs improvement. Jiang *et al.* [56] implemented an interesting thresholding scheme in which if the enhancing tumour is less than the set threshold, the region is substituted with necrosis instead, which might cause a significant improvement in the accuracy of the enhancing tumour class.

Certain limitations still exist in the current work. Firstly, the proposed segmentation ensemble is only evaluated on the official validation set of the challenge. The soundness of the method can be validated further by testing on separate clinical MRI data, independent of the challenge. Secondly, we did not extensively pre-process the dataset and post-process the results. Many reported models prepare their imaging data through intensity normalisation [63], [64] and bias correction [65] schemes to

minimise the variability in the data and make it analogous and comparable. Similarly, post-processing methods such as the use of conditional random fields [66] are shown to enhance segmentation accuracy. Further training on a larger dataset by extension of the input data through the inclusion of the BraTS 2016 dataset can also be employed, as it has been noted to improve the accuracy of models as demonstrated by Isensee *et al.* [46]. Nonetheless, the proposed ensemble exhibits efficient and robust tumour segmentation accuracies across multiple regions.

Further work can involve training on a larger dataset by expanding of the input data through the inclusion of the BraTS 2016 dataset, as it has been noted to improve the accuracy of models as demonstrated by Isensee *et al.* [46]. Additionally, extended training for more epochs can result in better generalization ability of the ensemble as well. In future, we also intend to add image processing (both pre- and post-processing) to the ensemble, along with further tuning of the hyperparameters.

CHAPTER 6

CONCLUSION

CONCLUSION

In this work, we have described an ensemble of two networks, both of which are individually used frequently on the task of biomedical image segmentation. The ensemble successfully generates highly accurate segmentation of brain tumours from the multimodal MRI scans as provided by the BraTS 2019 challenge, which compares favourably with predictions given from various other state of the art models. We use a method of variable ensembling to combine the respective outputs from the model to achieve the best scores. The proposed ensemble offers an automated and objective method of generating brain tumour segmentation to aid in disease planning and patient management clinically.

CHAPTER 7

REFERENCES

REFERENCES

[1] S. Bauer, R. Wiest, L. P. Nolte, and M. Reyes, "A survey of MRI-based medical image analysis for brain tumor studies," 2013.

[2] R. Leece, J. Xu, Q. T. Ostrom, Y. Chen, C. Kruchko, and J. S. Barnholtz-Sloan, "Global incidence of malignant brain and other central nervous system tumors by histology, 2003--2007," *Neuro. Oncol.*, vol. 19, no. 11, pp. 1553–1564, 2017.

[3] T. A. Dolecek, J. M. Propp, N. E. Stroup, and C. Kruchko, "CBTRUS statistical report: primary brain and central nervous system tumors diagnosed in the United States in 2005--2009," *Neuro. Oncol.*, vol. 14, no. suppl_5, pp. v1--v49, 2012.

[4] D. N. Louis *et al.*, "The 2016 World Health Organization classification of tumors of the central nervous system: a summary," *Acta Neuropathol.*, vol. 131, no. 6, pp. 803–820, 2016.

[5] R. Stupp *et al.*, "Radiotherapy plus concomitant and adjuvant temozolomide for glioblastoma," *N. Engl. J. Med.*, vol. 352, no. 10, pp. 987–996, 2005.

[6] S. Bakas *et al.*, "Identifying the best machine learning algorithms for brain tumor segmentation, progression assessment, and overall survival prediction in the BRATS challenge," *arXiv Prepr. arXiv1811.02629*, 2018.

[7] B. H. Menze, K. Van Leemput, D. Lashkari, M.-A. Weber, N. Ayache, and P. Golland, "A generative model for brain tumor segmentation in multi-modal images," in *International Conference on Medical Image Computing and Computer-Assisted Intervention*, 2010, pp. 151–159.

[8] S. Bakas *et al.*, "Advancing the cancer genome atlas glioma MRI collections with expert segmentation labels and radiomic features," *Sci. data*, vol. 4, p. 170117, 2017.

[9] S. Bakas *et al.*, "Segmentation labels and radiomic features for the pre-operative scans of the TCGA-LGG collection," *cancer imaging Arch.*, vol. 286, 2017.

[10] S. Bakas *et al.*, "Segmentation labels and radiomic features for the pre-operative scans of the TCGA-GBM collection. The Cancer Imaging Archive," *Nat Sci Data*, vol. 4, p. 170117, 2017.

[11] B. H. Menze *et al.*, "The multimodal brain tumor image segmentation benchmark (BRATS)," *IEEE Trans. Med. Imaging*, vol. 34, no. 10, pp. 1993–2024, 2014.

[12] S. Pereira, A. Pinto, V. Alves, and C. A. Silva, "Brain tumor segmentation using convolutional neural networks in MRI images," *IEEE Trans. Med. Imaging*, vol. 35, no. 5, pp. 1240–1251, 2016.

[13] R. Saouli, M. Akil, R. Kachouri, and others, "Fully automatic brain tumor segmentation using end-to-end incremental deep neural networks in MRI images," *Comput. Methods Programs Biomed.*, vol. 166, pp. 39–49, 2018.

[14] M. Goetz *et al.*, "DALSA: domain adaptation for supervised learning from sparsely

annotated MR images," *IEEE Trans. Med. Imaging*, vol. 35, no. 1, pp. 184–196, 2015.

[15] K. Farahani, B. Menze, and M. Reyes, "Brats 2014 Challenge Manuscripts (2014)," *URL http//www. braintumorsegmentation. org*, 2014.

[16] Y. Bengio, A. Courville, and P. Vincent, "Representation learning: A review and new perspectives," *IEEE Trans. Pattern Anal. Mach. Intell.*, vol. 35, no. 8, pp. 1798–1828, 2013.

[17] G. E. Hinton, S. Osindero, and Y.-W. Teh, "A fast learning algorithm for deep belief nets," *Neural Comput.*, vol. 18, no. 7, pp. 1527–1554, 2006.

[18] Y. Bengio, P. Lamblin, D. Popovici, and H. Larochelle, "Greedy layer-wise training of deep networks," in *Advances in neural information processing systems*, 2007, pp. 153–160.

[19] H. Lee, C. Ekanadham, and A. Y. Ng, "Sparse deep belief net model for visual area V2," in *Advances in neural information processing systems*, 2008, pp. 873–880.

[20] G. Wang, W. Li, T. Vercauteren, and S. Ourselin, "Automatic brain tumor segmentation based on cascaded convolutional neural networks with uncertainty estimation," *Front. Comput. Neurosci.*, vol. 13, p. 56, 2019.

[21] P. Mukherjee and A. Mukherjee, "Advanced processing techniques and secure architecture for sensor networks in ubiquitous healthcare systems," in *Sensors for Health Monitoring*, Elsevier, 2019, pp. 3–29.

[22] W. Chen, Y. Li, and C. Li, "A Visual Detection Method for Foreign Objects in Power Lines Based on Mask R-CNN," *Int. J. Ambient Comput. Intell.*, vol. 11, no. 1, pp. 34–47, 2020.

[23] P. C. Burger, E. R. Heinz, T. Shibata, and P. Kleihues, "Topographic anatomy and CT correlations in the untreated glioblastoma multiforme," *J. Neurosurg.*, vol. 68, no. 5, pp. 698–704, 1988.

[24] F. Raschke, T. R. Barrick, T. L. Jones, G. Yang, X. Ye, and F. A. Howe, "Tissue-type mapping of gliomas," *NeuroImage Clin.*, vol. 21, p. 101648, 2019.

[25] M. Soltaninejad, X. Ye, G. Yang, N. Allinson, T. Lambrou, and others, "Brain tumour grading in different MRI protocols using SVM on statistical features," 2014.

[26] M. Soltaninejad *et al.*, "Automated brain tumour detection and segmentation using superpixel-based extremely randomized trees in FLAIR MRI," *Int. J. Comput. Assist. Radiol. Surg.*, vol. 12, no. 2, pp. 183–203, 2017.

[27] M. Soltaninejad *et al.*, "Supervised learning based multimodal MRI brain tumour segmentation using texture features from supervoxels," *Comput. Methods Programs Biomed.*, vol. 157, pp. 69–84, 2018.

[28] T. L. Jones, T. J. Byrnes, G. Yang, F. A. Howe, B. A. Bell, and T. R. Barrick, "Brain tumor classification using the diffusion tensor image segmentation (D-SEG) technique," *Neuro. Oncol.*, vol. 17, no. 3, pp. 466–476, 2015.

[29] C. Galleguillos and S. Belongie, "Context based object categorization: A critical survey," *Comput. Vis. image Underst.*, vol. 114, no. 6, pp. 712–722, 2010.

[30] K. Kamnitsas *et al.*, "Efficient multi-scale 3D CNN with fully connected CRF for accurate brain lesion segmentation," *Med. Image Anal.*, vol. 36, pp. 61–78, 2017.

[31] F. Isensee, P. Kickingereder, W. Wick, M. Bendszus, and K. H. Maier-Hein, "Brain tumor segmentation and radiomics survival prediction: Contribution to the brats 2017 challenge," in *International MICCAI Brainlesion Workshop*, 2017, pp. 287–297.

[32] X. Li, H. Chen, X. Qi, Q. Dou, C.-W. Fu, and P.-A. Heng, "H-DenseUNet: hybrid densely connected UNet for liver and tumor segmentation from CT volumes," *IEEE Trans. Med. Imaging*, vol. 37, no. 12, pp. 2663–2674, 2018.

[33] F. Isensee, P. F. Jaeger, P. M. Full, I. Wolf, S. Engelhardt, and K. H. Maier-Hein, "Automatic cardiac disease assessment on cine-MRI via time-series segmentation and domain specific features," in *International workshop on statistical atlases and computational models of the heart*, 2017, pp. 120–129.

[34] K. Kamnitsas *et al.*, "Ensembles of multiple models and architectures for robust brain tumour segmentation," in *International MICCAI Brainlesion Workshop*, 2017, pp. 450–462.

[35] G. Wang, W. Li, S. Ourselin, and T. Vercauteren, "Automatic brain tumor segmentation using cascaded anisotropic convolutional neural networks," in *International MICCAI brainlesion workshop*, 2017, pp. 178–190.

[36] H. Dong, G. Yang, F. Liu, Y. Mo, and Y. Guo, "Automatic brain tumor detection and segmentation using U-Net based fully convolutional networks," in *annual conference on medical image understanding and analysis*, 2017, pp. 506–517.

[37] L. Fidon *et al.*, "Scalable multimodal convolutional networks for brain tumour segmentation," in *International Conference on Medical Image Computing and Computer-Assisted Intervention*, 2017, pp. 285–293.

[38] T. H. N. Le, R. Gummadi, and M. Savvides, "Deep recurrent level set for segmenting brain tumors," in *International Conference on Medical Image Computing and Computer-Assisted Intervention*, 2018, pp. 646–653.

[39] Y. Qin *et al.*, "Autofocus layer for semantic segmentation," in *International Conference on Medical Image Computing and Computer-Assisted Intervention*, 2018, pp. 603–611.

[40] H. Shen, R. Wang, J. Zhang, and S. J. McKenna, "Boundary-aware fully convolutional network for brain tumor segmentation," in *International Conference on Medical Image Computing and Computer-Assisted Intervention*, 2017, pp. 433–441.

[41] S. Pereira, V. Alves, and C. A. Silva, "Adaptive feature recombination and recalibration for semantic segmentation: application to brain tumor segmentation in MRI," in *International Conference on Medical Image Computing and Computer-Assisted Intervention*, 2018, pp. 706–714.

[42] C. Zhou, C. Ding, Z. Lu, X. Wang, and D. Tao, "One-pass multi-task convolutional

neural networks for efficient brain tumor segmentation," in *International Conference on Medical Image Computing and Computer-Assisted Intervention*, 2018, pp. 637–645.

[43] Z. Ji, Y. Shen, C. Ma, and M. Gao, "Scribble-based hierarchical weakly supervised learning for brain tumor segmentation," in *International Conference on Medical Image Computing and Computer-Assisted Intervention*, 2019, pp. 175–183.

[44] H. Xu, H. Xie, Y. Liu, C. Cheng, C. Niu, and Y. Zhang, "Deep cascaded attention network for multi-task brain tumor segmentation," in *International Conference on Medical Image Computing and Computer-Assisted Intervention*, 2019, pp. 420–428.

[45] A. Myronenko, "3D MRI brain tumor segmentation using autoencoder regularization," in *International MICCAI Brainlesion Workshop*, 2018, pp. 311–320.

[46] F. Isensee, P. Kickingereder, W. Wick, M. Bendszus, and K. H. Maier-Hein, "No new-net," in *International MICCAI Brainlesion Workshop*, 2018, pp. 234–244.

[47] R. McKinley, R. Meier, and R. Wiest, "Ensembles of densely-connected CNNs with label-uncertainty for brain tumor segmentation," in *International MICCAI Brainlesion Workshop*, 2018, pp. 456–465.

[48] C. Zhou, S. Chen, C. Ding, and D. Tao, "Learning contextual and attentive information for brain tumor segmentation," in *International MICCAI Brainlesion Workshop*, 2018, pp. 497–507.

[49] G. K. Murugesan *et al.*, "Multidimensional and Multiresolution Ensemble Networks for Brain Tumor Segmentation," in *International MICCAI Brainlesion Workshop*, 2019, pp. 148–157.

[50] C. Chen, X. Liu, M. Ding, J. Zheng, and J. Li, "3D dilated multi-fiber network for real-time brain tumor segmentation in MRI," in *International Conference on Medical Image Computing and Computer-Assisted Intervention*, 2019, pp. 184–192.

[51] P. Yun, L. Tai, Y. Wang, C. Liu, and M. Liu, "Focal loss in 3d object detection," *IEEE Robot. Autom. Lett.*, vol. 4, no. 2, pp. 1263–1270, 2019.

[52] R. Hua *et al.*, "Segmenting Brain Tumor Using Cascaded V-Nets in Multimodal MR Images," *Front. Comput. Neurosci.*, vol. 14, 2020.

[53] C. H. Sudre, W. Li, T. Vercauteren, S. Ourselin, and M. J. Cardoso, "Generalised dice overlap as a deep learning loss function for highly unbalanced segmentations," in *Deep learning in medical image analysis and multimodal learning for clinical decision support*, Springer, 2017, pp. 240–248.

[54] F. Milletari, N. Navab, and S.-A. Ahmadi, "V-net: Fully convolutional neural networks for volumetric medical image segmentation," in *2016 fourth international conference on 3D vision (3DV)*, 2016, pp. 565–571.

[55] A. A. Novikov, D. Lenis, D. Major, J. Hlad\uuvka, M. Wimmer, and K. Bühler, "Fully convolutional architectures for multiclass segmentation in chest radiographs," *IEEE Trans. Med. Imaging*, vol. 37, no. 8, pp. 1865–1876, 2018.

[56] Z. Jiang, C. Ding, M. Liu, and D. Tao, "Two-Stage Cascaded U-Net: 1st Place Solution to BraTS Challenge 2019 Segmentation Task," in *International MICCAI Brainlesion Workshop*, 2019, pp. 231–241.

[57] Y.-X. Zhao, Y.-M. Zhang, and C.-L. Liu, "Bag of Tricks for 3D MRI Brain Tumor Segmentation," in *International MICCAI Brainlesion Workshop*, 2019, pp. 210–220.

[58] R. McKinley, M. Rebsamen, R. Meier, and R. Wiest, "Triplanar Ensemble of 3D-to-2D CNNs with Label-Uncertainty for Brain Tumor Segmentation," in *International MICCAI Brainlesion Workshop*, 2019, pp. 379–387.

[59] M. Hamghalam, B. Lei, and T. Wang, "Brain tumor synthetic segmentation in 3D multimodal MRI scans," in *International MICCAI Brainlesion Workshop*, 2019, pp. 153–162.

[60] M. Frey and M. Nau, "Memory efficient brain tumor segmentation using an autoencoder-regularized U-Net," in *International MICCAI Brainlesion Workshop*, 2019, pp. 388–396.

[61] Y. Xue *et al.*, "A multi-path decoder network for brain tumor segmentation," in *International MICCAI Brainlesion Workshop*, 2019, pp. 255–265.

[62] A. Myronenko and A. Hatamizadeh, "Robust semantic segmentation of brain tumor regions from 3d mris," in *International MICCAI Brainlesion Workshop*, 2019, pp. 82–89.

[63] M. Goetz, C. Weber, J. Bloecher, B. Stieltjes, H.-P. Meinzer, and K. Maier-Hein, "Extremely randomized trees based brain tumor segmentation," *Proceeding of BRATS challenge-MICCAI*, pp. 6–11, 2014.

[64] X. Zhao, Y. Wu, G. Song, Z. Li, Y. Zhang, and Y. Fan, "A deep learning model integrating FCNNs and CRFs for brain tumor segmentation," *Med. Image Anal.*, vol. 43, pp. 98–111, 2018.

[65] N. J. Tustison *et al.*, "N4ITK: improved N3 bias correction," *IEEE Trans. Med. Imaging*, vol. 29, no. 6, pp. 1310–1320, 2010.

[66] S. Bauer, T. Fejes, J. Slotboom, R. Wiest, L.-P. Nolte, and M. Reyes, "Segmentation of brain tumor images based on integrated hierarchical classification and regularization," in *MICCAI BraTS Workshop. Nice: Miccai Society*, 2012, p. 11.

ORIGINALITY REPORT

14%	1%	15%	4%
SIMILARITY INDEX	INTERNET SOURCES	PUBLICATIONS	STUDENT PAPERS

PRIMARY SOURCES

1	"Brainlesion: Glioma, Multiple Sclerosis, Stroke and Traumatic Brain Injuries", Springer Nature, 2019 Publication	4%
2	"Brainlesion: Glioma, Multiple Sclerosis, Stroke and Traumatic Brain Injuries", Springer Science and Business Media LLC, 2020 Publication	4%
3	"Brainlesion: Glioma, Multiple Sclerosis, Stroke and Traumatic Brain Injuries", Springer Science and Business Media LLC, 2018 Publication	1%
4	"Medical Image Computing and Computer Assisted Intervention – MICCAI 2018", Springer Science and Business Media LLC, 2018 Publication	1%
5	"Medical Image Computing and Computer Assisted Intervention – MICCAI 2019", Springer Science and Business Media LLC, 2019 Publication	1%

6	academic.oup.com Internet Source	1%
7	www.wjgnet.com Internet Source	1%
8	"Statistical Atlases and Computational Models of the Heart. Atrial Segmentation and LV Quantification Challenges", Springer Science and Business Media LLC, 2019 Publication	<1%
9	Mina Ghaffari, Arcot Sowmya, Ruth Oliver. "Automated Brain Tumor Segmentation Using Multimodal Brain Scans: A Survey Based on Models Submitted to the BraTS 2012–2018 Challenges", IEEE Reviews in Biomedical Engineering, 2020 Publication	<1%
10	Submitted to University of Sydney Student Paper	<1%
11	"Radiomics and Radiogenomics in Neuro-oncology", Springer Science and Business Media LLC, 2020 Publication	<1%
12	Submitted to Higher Education Commission Pakistan Student Paper	<1%

13	Internet Source	<1%

Exclude quotes	Off	Exclude matches	Off
Exclude bibliography	On		